26th INTERNATIONAL CONGRESS ON SOUND AND VIBRATION
7-11 July 2019, Montreal

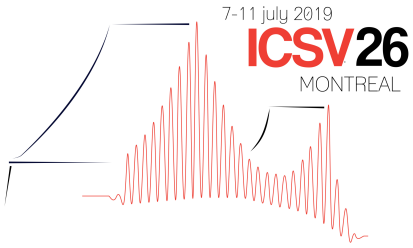

ON THE NUMERICAL MODELLING OF REVERBERATION ROOMS, INCLUDING A COMPARISON WITH EXPERIMENTS

N.B. Roozen
KU Leuven, Laboratory of Acoustics, Department of Physics, Celestijnenlaan 200D, Leuven, Belgium
email: bert.roozen@kuleuven.be

E.A. Piana
Università degli Studi di Brescia, Applied Acoustics Laboratory, Via Branze 38, Brescia, Italy

E. Deckers
KU Leuven, Department of Mechanical Engineering, Celestijnenlaan 300, Leuven, Belgium
DMMS lab, Flanders Make

C. Scrosati
ITC-CNR, Laboratory of Acoustics, Via Lombardia 49 - 20098 San Giuliano Milanese, Milan, Italy

At low frequencies the acoustic field in a reverberation room is not diffuse, and it should therefore be modeled by means of a deterministic approach. In this work, a finite element model was developed to include the modal behavior of the room. Dissipation in the empty reverberation room is taken into account by means of a volumetric approach, using an explicit closed-form expression for the complex speed of sound, on the basis of standard reverberation time measurements. Comparisons with measurements in a reverberation room show that the transfer functions and impulse response functions can be predicted fairly well.

Keywords: Room acoustics, low frequency sound absorption, reverberation room, numerical modelling.

1. Introduction

Within the context of the Round Robin Test on low frequency sound absorption measurements in reverberation rooms and impedance tubes (see the accompanying paper [1]), being part of the DENORMS COST action CA15125, time history measurements were performed in the reverberation room of the Acoustics Laboratory - KU Leuven. The reverberation room was tested in different configurations, but for the purpose of the present paper only the empty case, with diffusers and without absorption sample, will be considered. Several loudspeaker and microphone positions were used during the experiments for this purpose. Details of the test set-up are described in Section 2.

A numerical model of this reverberation room was created to obtain a better understanding of the measured phenomena, with an emphasis on frequencies below 100 Hz. The model is described in Section 3.1. This paper discloses some preliminary results that were obtained by the numerical model. The results are compared with the experiments in Section 3.3.

2. Experimental test set-up

The measurements described in this paper were performed in a reverberation room with a volume of 197 m^3. The lateral dimensions are approximately $8 \times 7 \times 4$ meters. None of the walls in this reverberation room are parallel to each other. Whilst two walls are running vertically, the two other opposing walls are tilted (i.e. do not have an angle of 90 degrees with the horizontal floor surface). The ceiling of the room consists of two parts, which are also non-parallel to the (horizontal) floor. A drawing of the reverberation room is given in Fig. 1. Five diffusers were mounted in room, as shown in Fig. 2.

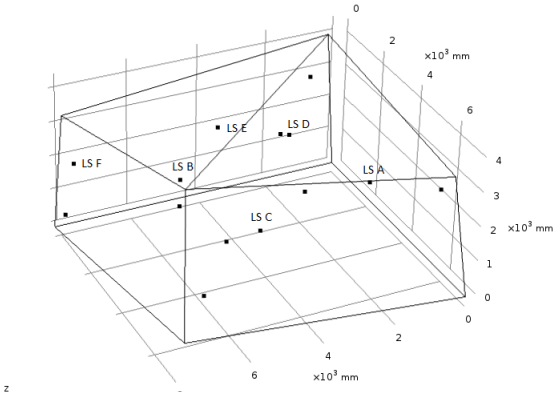

A)

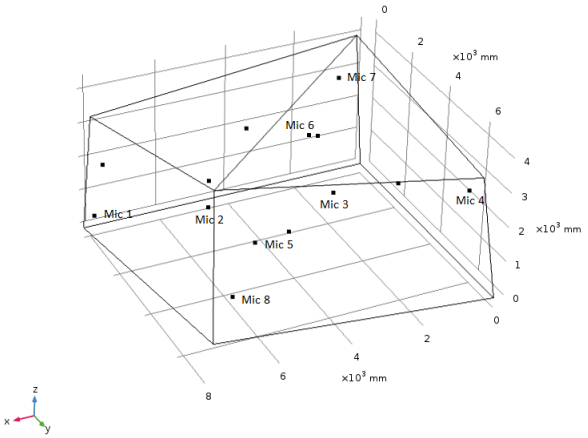

B)

Figure 1: A): Loudspeaker positions in the room, all at a height of 2.12 m. B): Microphone positions in the room, along two diagonals.

In total 6 loudspeaker positions were used in the tests. Their positions, labeled from "A" through "F", are shown in Fig. 1A. The acoustic response was measured at 8 different positions, labeled "Mic1" through "Mic8" in Fig. 1B.

An omni-directional loudspeaker, Bruel & Kjaer type 4295, was used as sound source (see Fig. 2A). This loudspeaker radiates sound through a conical coupler to a circular orifice.

Two types of microphones were used (see Fig. 2B): 5 microphones from BSWA, type 201, with preamplifier type MA201, and 3 microphones from Bruel & Kjaer type 4189 with preamplifier type 2671.

Using a logarithmic sweep excitation signal from 20 Hz to 5 kHz, transfer functions were computed between the 8 microphones, for each position of the loudspeaker. A 9th microphone was placed near the orifice of the loudspeaker to characterize its emissions (see Fig. 2C). The autopower spectra and the transfer functions between the microphones have been used to validate the numerical simulations. These comparisons will be discussed in Section 3.

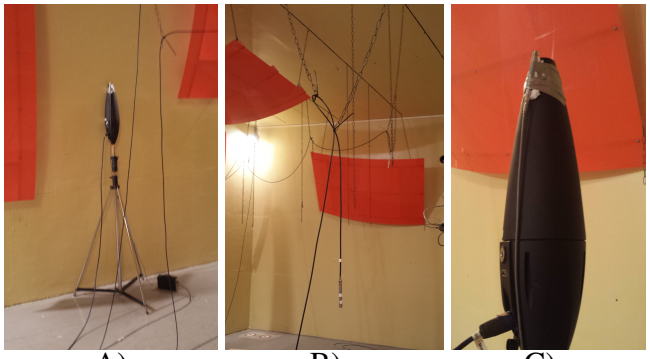

A) B) C)

Figure 2: Measurement equipment inside the reverberation room with diffusers (orange panels) A): Loudspeaker Bruel & Kjaer type 4295. B): One of the suspended microphones. C): Microphone placed near the orifice of the loudspeaker Bruel & Kjaer type 4295.

The post-processing was performed on the time domain data (see the accompanying paper [2]) to obtain the reverberation time as a function of frequency. The resulting average T20 is shown in Fig. 3.

3. Numerical simulations

3.1 Model description

The finite element model is depicted in Fig. 4. It consists of 18281 tetrahedral elements, resulting in

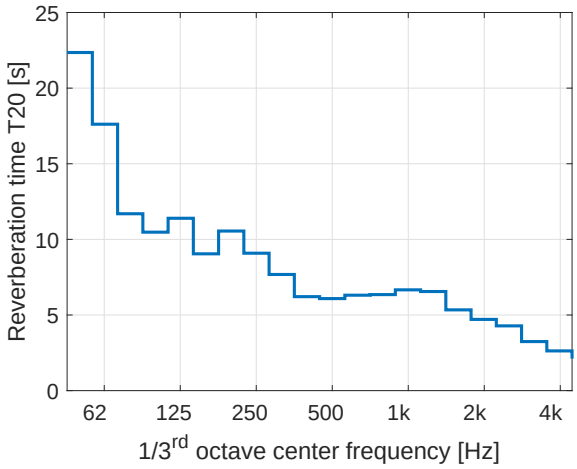

Figure 3: Measured reverberation time

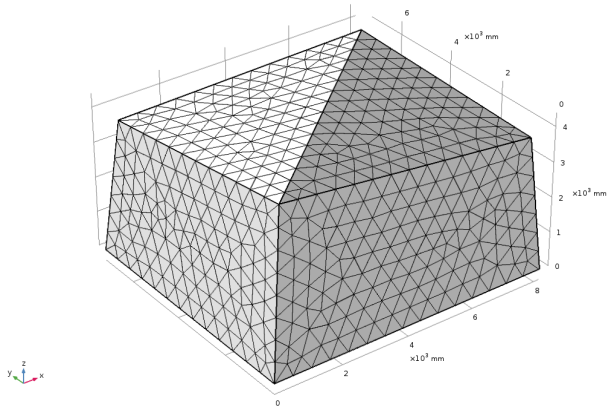

Figure 4: The finite element mesh of the reverberation room.

26183 degrees of freedom. The maximum element size is approximately 220 mm, allowing acoustic simulations to be performed up to c/λ=340/(0.22*6) ≈250 Hz (6 elements per wavelength λ). The frequency response simulations (specifying a complex speed of sound, see Section 3.2) required approximately 15 minutes of computation time for 652 response frequencies on an Intel i7 CPU running at 3.4 GHz. The eigenmode analysis, computing all 37 modes up to 100 Hz, required also about 15 minutes of CPU time. All walls are defined as acoustically hard. The acoustic losses in the room are accounted for by means of a frequency dependent, complex speed of sound, as described in the next section. The diffusers were not physically modelled. The omission of the diffusers in the model is considered to be correct at low frequencies, as the acoustic wavelength is much longer than the dimensions of the diffusers.

3.2 Incorporation of the losses in the reverberation room model on the basis of reverberation time measurements

Despite the commonly accepted belief that at low frequencies the dissipation of the energy of acoustic energy is mainly occurring at the walls of a room, a volumetric approach is applied in this paper to account for the absorption effects in the empty reverberation room. Dissipative effects are uniformly distributed over the whole volume of the reverberation room. The advantage of this approach is that it is relatively simple. Closed-form expressions can be used to account for the dissipation in the room. There is no need for a cumbersome reconstruction of the wall impedances from implicit relationships, as in [3].

From the measurement data, an estimation of the reverberation time was obtained (see the accompanying paper [2]). Having knowledge about the reverberation time RT, the loss factor of the whole volume of the room η can be determined by means of the following well known formula:

$$\eta = \frac{2.2}{f\ RT} \tag{1}$$

where f is the frequency. By means of the loss factor η, a complex bulk modulus $K = K_0\,(1 + i\eta)$ can be computed, resulting in a complex speed of sound which is given by

$$c = \sqrt{\frac{K}{\rho}} = \sqrt{\frac{K_0\,(1 + i\eta)}{\rho}} \tag{2}$$

where ρ is the density of air. For small values of η, this relationship simplifies to

$$c \approx c_0\,(1 + 0.5i\eta) = c_0\left(1 + 0.5i\frac{2.2}{f\ RT}\right) \tag{3}$$

with $c_0 = \sqrt{\frac{K_0}{\rho}}$

The exact expression in Eq. 2 or the approximate expression in Eq. 3 gives a frequency dependent, complex speed of sound that takes into account the actual losses in the room.

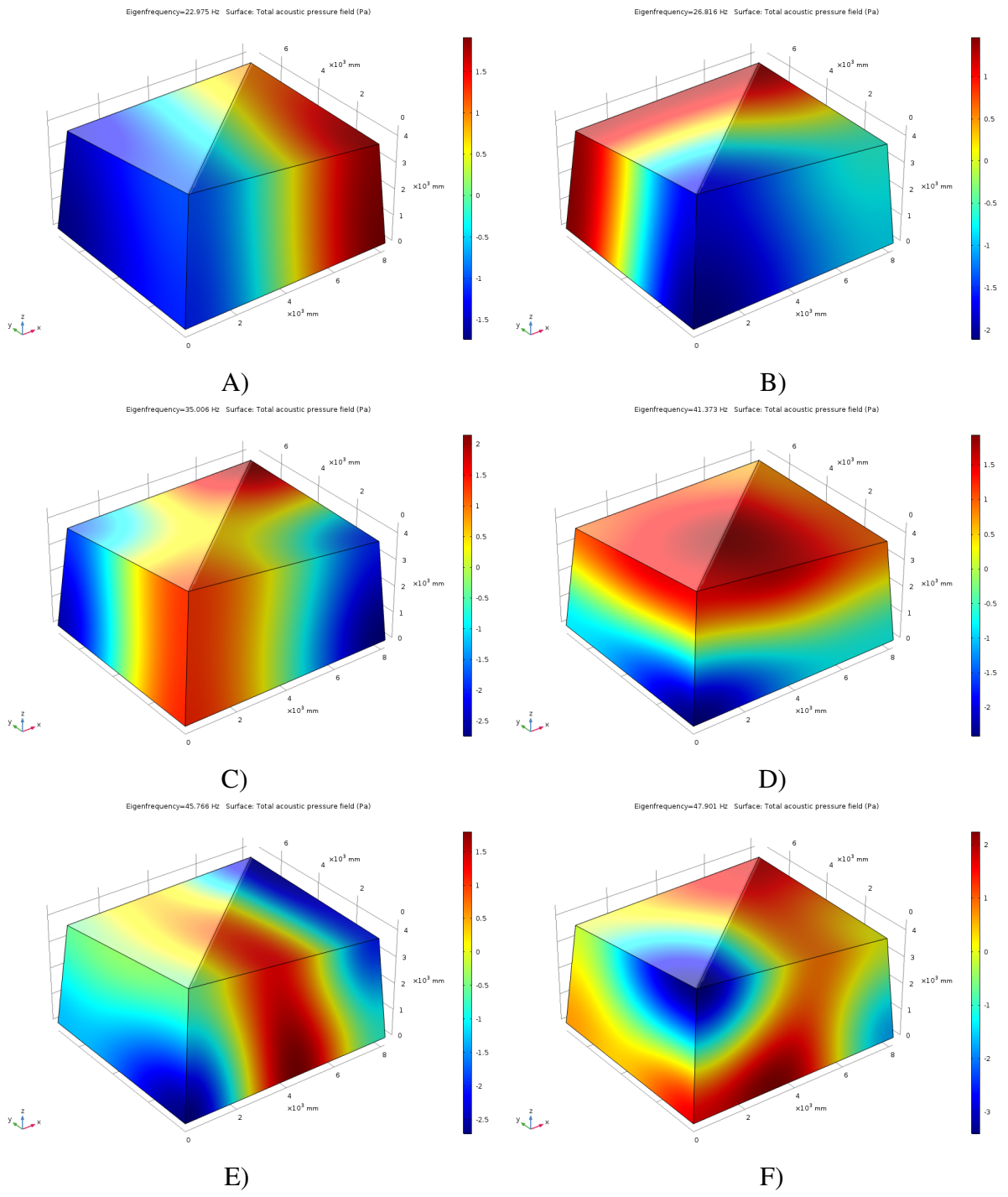

Figure 5: Acoustic eigenmodes 1 to 6. A): mode 1, 23.0 Hz, B): mode 2, 26.8 Hz, C): mode 3, 35.0 Hz, D): mode 4, 41.4 Hz, E): mode 5, 45.8 Hz, F): mode 6, 47.9 Hz.

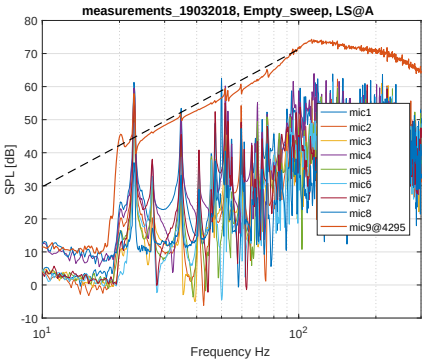

A)

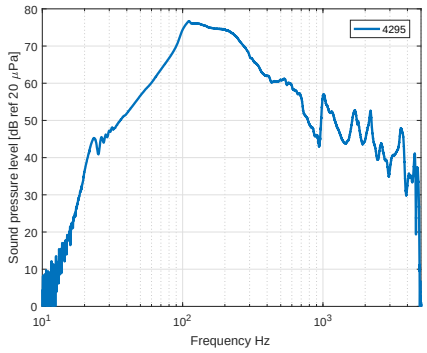

B)

Figure 6: Measured acoustic response functions of the loudspeaker Bruel & Kjaer type 4295. A): in the reverberation room, together with all other microphone channels. The dotted black line indicates a slope of approximately 40 dB/dec. B): in the anechoic room.

3.3 Numerical results and comparison with experiments

The first 6 eigenmodes of the room are depicted in Fig. 5. The lowest eigenfrequency of this room is 23 Hz.

The easiest way to compare the measured data with the numerical model is to verify that the computed eigenfrequencies correspond to the peaks in the autopower spectra. Figures 7, 8 and 9 show the numerically predicted acoustic response functions for microphone positions 2, 4 and 7, respectively, with the loudspeaker at position A.

In the numerical model, an ideal point source with a volumetric flow rate of 1 l/s was used at the loudspeaker positions. During the measurements a Bruel & Kjaer power amplifier type 2718 powered the omnidirectional loudspeaker, driving it with a constant voltage. From measurements of the microphone near the orifice of the omnidirectional loudspeaker (the 9th microphone, see Fig. 2C)), it became clear that, for frequencies below 100 Hz, the sound pressure in the room increased by approximately 40 dB/dec, as shown in Fig. 6A.

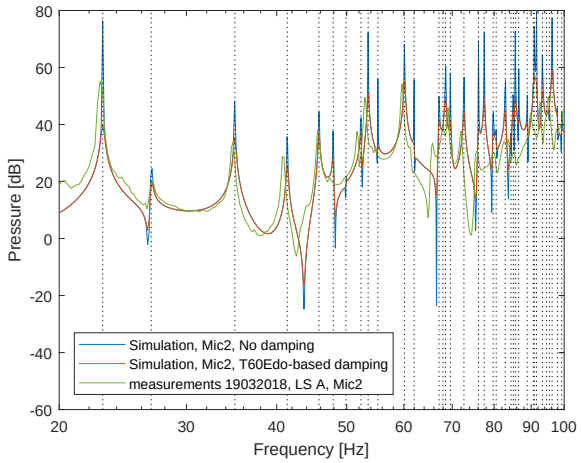

Figure 7: Numerically predicted and measured acoustic response functions for microphone positions 2, loudspeaker position A. The vertical dashed lines indicate the numerically predicted acoustic resonance frequencies.

The sound pressure level of the Bruel & Kjaer omnidirectional loudspeaker type 4295 was also measured in an anechoic room with a gross volume of 289 m^3 and a net volume of 120 m^3 at a distance of a few cm from the orifice. The results are shown in Fig. 6B.

From Fig. 6B it can be seen that the acoustic resonances internal to the Bruel & Kjaer omnidirectional loudspeaker type 4295 do not occur in the frequency range of interest. Knowing this, the ripples of the sound pressure level of the reference microphone near the orifice of the loudspeaker (Fig. 6A) can only be attributed to a change of impedance at the resonance frequencies of the reverberation room. Especially the ripple at a frequency of 23 Hz, the first resonance frequency of the reverberation room, is rather strong. The other ripples are less strong, allowing to scale the radiated sound power of the loudspeaker by the 40 dB/dec approximation.

Thus, to compare the numerically generated response functions with the experimentally determined ones, the results from the numerical model need to be scaled by a constant factor (to account for the un-

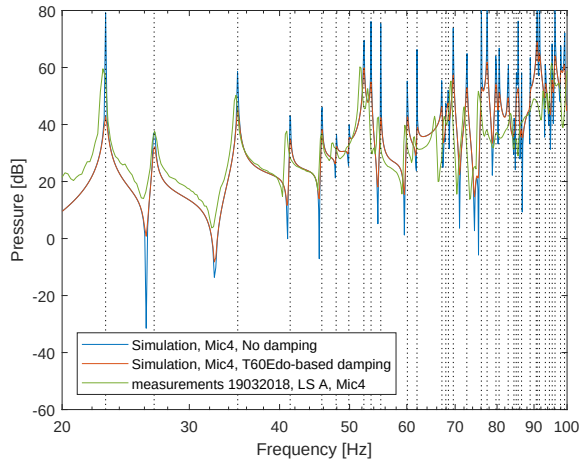

Figure 8: Numerically predicted and measured acoustic response functions for microphone positions 4, loudspeaker position A. The vertical dashed lines indicate the numerically predicted acoustic resonance frequencies.

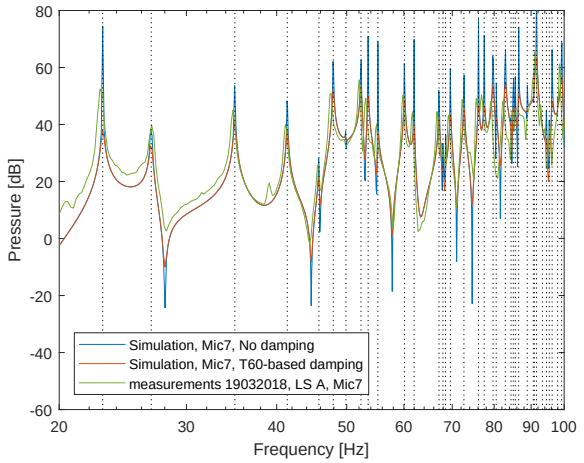

Figure 9: Numerically predicted and measured acoustic response functions for microphone positions 7, loudspeaker position A. The vertical dashed lines indicate the numerically predicted acoustic resonance frequencies.

known gain of the amplifier) and with an additional 40 dB/dec shift. The results are shown in Figs. 7, 8 and 9 for microphone positions 2, 4 and 7, together with the experimentally determined response functions. The correspondence between the numerical predictions and the measurements is very satisfactory.

An additional comparison was carried out by considering the ratio (i.e. the transfer function) of the sound pressure at two microphone positions. Figs. 10, 11 and 12 show the transfer functions between microphone positions 4-2, positions 7-2 and positions 7-4, respectively. For this comparison, the results do not need to be scaled. As can be seen from these figures, also the predicted transfer functions and the measured ones compare very well with each other.

In both cases (i.e. for the absolute sound pressure levels shown in Figs. 7-9 and the transfer functions shown in Figs. 10-12) it is mandatory to specify the correct amount of damping. The proposed procedure to take the reverberation time measurement data as a basis to construct a complex speed of sound (see Section 3.2), proves to be a good approach. Note that in case no damping is specified at all in the numerical model, as in the blue curves in Figs. 7-12, the peaks and valleys are way too high, or too deep, respectively.

Murillo et al. [3] model the dissipative effects in a room at low frequencies (typically < 100 Hz) by means of a complex impedance on the walls. They observe a frequency shift of the resonant peaks due to a non-zero reactance (i.e. the imaginary part of the impedance), resulting in a better correspondence of the predicted and measured resonance peaks. In this work, the necessity to specify a non-zero reactance is not that apparent. Modeling the reverberation room walls as hard wall boundaries, using the actual geometry of the room, and modeling the dissipation in the room by means of a volumetric approach (Section 3.2) yields a satisfactory correspondence between predicted and measured resonance frequencies as shown in the Figs. 7-12.

Knowing the (numerically predicted) transfer functions, the time domain impulse response functions can be obtained by means of an inverse Fourier transform. To demonstrate this capability, a numerical simulation was performed from DC up to 125 Hz, in steps of $df = 0.1$ Hz. Applying an inverse Fourier transform yields a time domain signal with a length of $T = 10$ seconds ($T = 1/df$). The impulse response is considered for microphone #2 and loudspeaker position A. In Fig. 13, the impulse response was filtered keeping the frequency content of the numerically generated data between 53 Hz and 62 Hz, which contains two resonance frequencies. The nu-

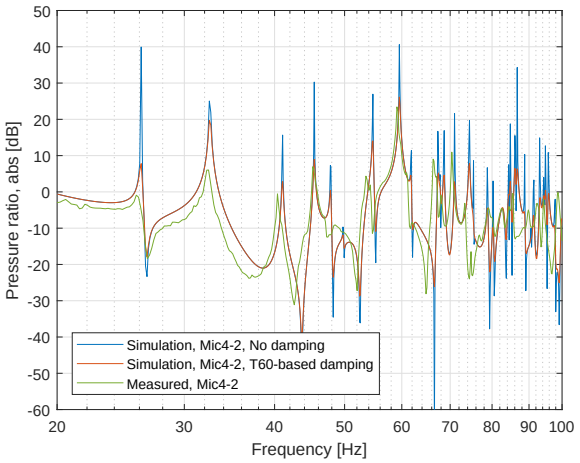

Figure 10: Numerically predicted and measured acoustic transfer functions between microphone positions 2 and 4, for loudspeaker position A.

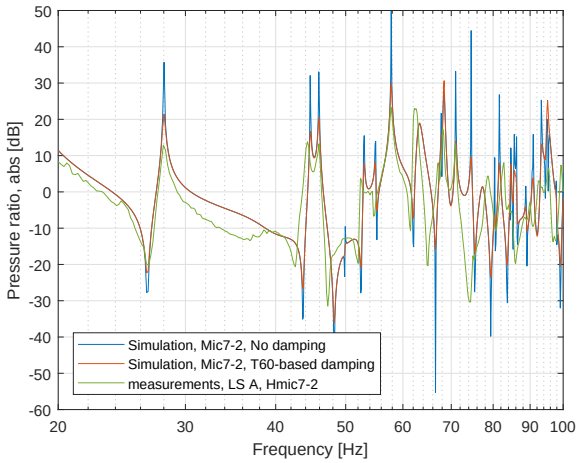

Figure 11: Numerically predicted and measured acoustic transfer functions between microphone positions 2 and 7, for loudspeaker position A.

merically computed frequency data outside this frequency range were zeroed. The beating effects of the two eigenmodes of the room are clearly visible.

A comparison of numerically generated impulse responses with experimentally obtained impulse responses in the time domain is difficult, as the phase of the loudspeaker and of the amplifier varies strongly as function of frequency, and it is usually unknown. If such a comparison is required, this phase information should be measured.

4. Conclusions

The numerically predicted transfer functions between microphones and the numerically predicted impulse response functions of an empty reverberation room were compared with experimental data. The dissipation of the acoustic waves was taken into account by means of a volumetric approach, using a complex speed of sound. The imaginary part of the complex speed of sound was estimated from the measured reverberation time by means of simple closed-form expressions. The correspondence between the numerically predicted transfer functions and the transfer functions derived from the measured impulse response functions was satisfactory. The resonance frequencies were predicted correctly, as well as the absolute values of the transfer functions.

In the present work the sound pressure close to the orifice of the loudspeaker was taken as a reference to scale the impulse response functions at the microphone positions. For future work it is recommended to measure in-situ the power being emitted by the loudspeaker by means of a two-microphone approach.

5. Acknowledgments

This article is based upon work from COST Action DENORMS CA15125, supported by COST (European Cooperation in Science and Technology). The research of E. Deckers is funded by a postdoctoral grant from the Research Foundation - Flanders (FWO). The research of N.B. Roozen was supported by the H2020-MSCA-RISE-2015 project No. 690970 Papabuild. During this project the COMSOL Multiphysics version 5.4 license of the University of Brescia was used.

REFERENCES

1. Scrosati, C., Roozen, N.B. and Piana, E.A., Principles at the basis of the DENORMS round robin test on the low frequency sound absorption measurements in reverberation rooms and impedance tube, *Proceedings of the 26th International Congress on Sound and Vibration*, Montréal, Canada, 7-11 July, (2019).

2. Piana, E.A., Roozen, N.B. and Scrosati, C. The DENORMS Round Robin Test: measurement procedure and post-processing of time data, *Proceedings of the 26th International Congress on Sound and Vibration*, Montréal, Canada, 7-11 July, (2019).

3. Murillo, D. M., Fazi, F. M. and Astley, J. Room Acoustic Simulations Using the Finite Element Method and Diffuse Absorption Coefficients, *Acta Acustica united with Acustica*, **105**(1), 231–239, (2019).

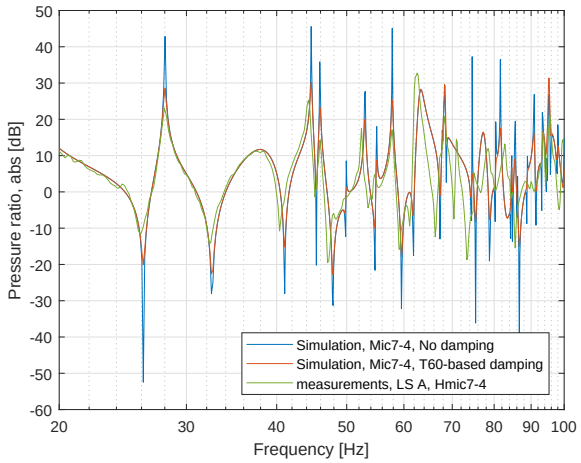

Figure 12: Numerically predicted and measured acoustic transfer functions between microphone positions 4 and 7, for loudspeaker position A.

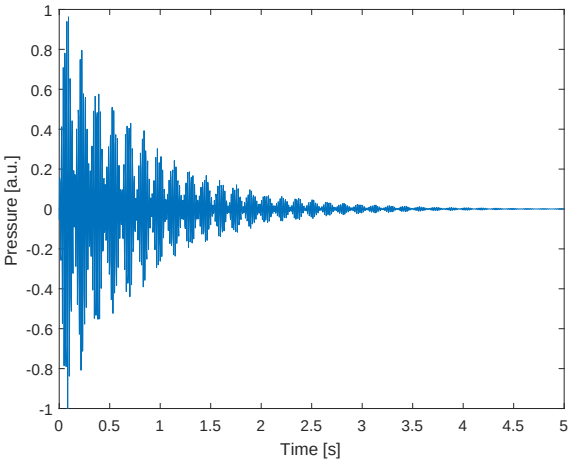

Figure 13: Time domain impulse response, constructed by means of inverse Fourier transform of numerically generated frequency response data. Frequency spectrum filtered with a bandpass filter from 52 Hz to 62 Hz. Loudspeaker position A, microphone position 2, T60-based damping with diffusers.